PNAS COMMENTARY

Honing in on the climate signal in seafloor topography

Garrett Ito[a,1]

The corrugated surface of the seafloor expresses the most areally extensive landform on Earth, known as "abyssal hills", inherited from when the oceanic crust was created at a midocean ridge spreading center (1, 2) (Fig. 1). The main process is the shifting and rotation of adjacent blocks of crust relative to one another along fault zones predominantly during periods of low magmatic activity, interspersed between times of robust magmatism and the emplacement new crust (1, 3). In the presence of the steady far-field tug of plate tectonic forces, this interplay between faulting and magmatism depends on processes influencing the time dependence of magma generation, storage, and delivery to the surface (4, 5). In PNAS, Huybers et al. (6) argue that one such process originates with the fall and rise of sea level during glacial–interglacial climate cycles.

Glacial–interglacial climate fluctuations have been linked to changes in eruptive output at subaerial volcanoes through the changes in the surface loading of ice mass (7–9). There is also mounting evidence in the marine sediment record that magmatic activity at midocean ridges has correlated in time with climate cycles (10, 11). Numerical model simulations predict that changes in sea-level induced pressure variations on the seafloor are transmitted to the underlying mantle where they can lead to fluctuations in the amount of magma produced (10, 12). This can be understood when considering the fact that magmatism at midocean ridges is fed primarily by the pressure-release partial melting that occurs as (hot) mantle rises in response to the spreading of the overlying (relatively cool) lithospheric plates. This continual pressure-release melting stabilizes a layer, ∼80 km in thickness, that is right at its melting-point temperature and pressure. Although the pressure variation due to the estimated ∼100 m of sea level change is relatively small across this layer, the change occurs over geologically short timescales (10° ky to 10^{1} ky), so the rate of pressure change can perturb the flux of decompression melting by an appreciable fraction (∼10%).

The search for the hypothesized climate signal in seafloor topography has proven challenging. Goff's (13) analysis of high-resolution, seafloor topography data collected using shipboard sonar instruments failed to show statistically significant variability in topography with seafloor age near three midocean ridges. These findings indicate that the climate signal—if present—is insufficiently coherent in time in those areas, or is below the temporal resolution availed by the data. Other studies have found undulations in seafloor topography corresponding to the dominant periods associated with Milankovitch cycles of 100, 41, and 23 ky (12, 14–16). Those findings, however, were in a few very localized areas, whereas the climate phenomenon is global and should impact many areas broadly. Furthermore, the reliance on single or few shipboard measurement profiles can be problematic (12) because local variability can cause the results to be sensitive to the choice of profile examined (17).

Huybers et al. (6) provide an important advancement by examining >200 shipboard profiles in 17 different areas representing an appreciable range of seafloor spreading environments around the globe. Their results fortify prior findings (18) for the dominant global tendency of the characteristic wavelengths of abyssal hills to decrease with increasing seafloor spreading rate, a relation that opposes the positive correlation expected for climate control and, instead, reflects the first-order controls of lithosphere structure and magma flux as they differ with spreading rate (19) (Fig. 1). However, with more detailed scrutiny, Huybers et al. (6) highlight subsidiary positive trends in abyssal hill wavelengths when the data are grouped by spreading rate. At intermediate (2.3 cm/y to 3.8 cm/y) rates, abyssal hill wavelength tends to increase with spreading rate, with a best-fitting slope close to that expected for the 100-ky Milankovitch period. At fast (>3.8 cm/y) spreading rates, the best-fitting positive slope is close to that expected for the 41-ky Milankovitch period (see also ref. 20).

Furthermore, seafloor ages determined from seafloor magnetic isochrons enabled the observations of topography in space to be analyzed as variations in time in the spectral domain (6) . The 100-ky period for seafloor formed at the intermediate spreading rates produced nonconclusive results, perhaps because lithosphere thickness controls on faulting are expected to produce topography at similar frequencies at intermediate spreading rates (17). In contrast, the 41-ky signal identified in the spatial domain near fast-spreading midocean ridges is distinguished as a statistically significant peak in spectral power at frequencies near 1/41 ky^{-1}.

The second key advancement Huybers et al. (6) make is a mechanics-based explanation for causes of the observations. Computer calculations simulate the spreading of two lithospheric plates in the presence of episodes of magmatically accommodated extension, interspersed with periods of magmatic quiescence and fault-accommodated extension. For a given spreading rate, when the period spanning the full magmatic–amagmatic cycle is below a

Author affiliations: [a]Department of Earth Sciences, University of Hawai'i at Mānoa, Honolulu, HI 96822

Author contributions: G. I. analyzed data and wrote the paper.

The author declares no competing interest.

See companion article, "Influence of Late Pleistocene sea level variations on midocean ridge spacing in faulting simulations and a global analysis of bathymetry," 10.1073/pnas.2204761119.

[1]Email: gito@hawaii.edu.

Published July 26, 2022.

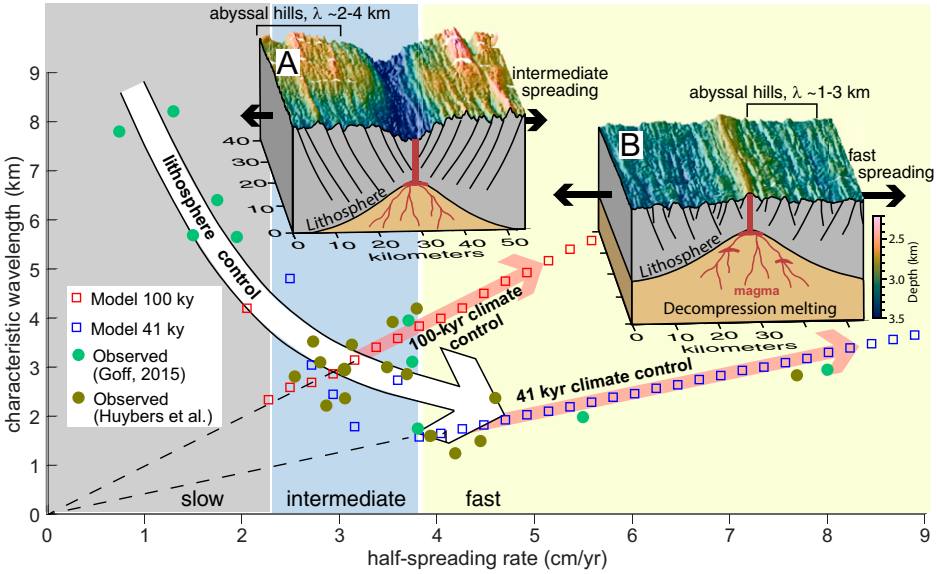

Fig. 1. Modified from Huybers et al. (6), showing observed (colored circles) and modeled (open squares) characteristic wavelengths of abyssal hill topography versus the rate of seafloor spreading. When considering all of the observations together, wavelength correlates negatively with spreading rate (17,18,20). The models by Huybers et al. (6) confirm findings of previous studies that this negative correlation reflects "lithospheric controls" (large white arrow) on fault wavelength when the periods of magmatic and amagmatic cycles are relatively short (19). However, when observations at intermediate spreading rates and fast spreading rates are viewed as two separate groups, the wavelengths within each group correlate positively with spreading rate (19, 21). The models predict this to reflect the climate control on fault wavelength. The Milanovitch period of 100 ky is predicted to control fault wavelengths at intermediate and greater spreading rates, whereas the Milankovitch period of 41 ky is predicted to control fault wavelengths only at fast spreading rates. *Insets* show 3D perspective views of seafloor topography at (inset A) the Chile Ridge and (inset B) the East Pacific Rise. Cartoons on the front panels depict the cool, stiff lithosphere (gray) that deforms by faulting (solid lines), as well as the hot underlying layer (orange) where magma (red) is created by pressure release melting. Wavelengths, λ, of abyssal hill topography as labeled are taken from the observations in the main plot.

threshold value, the predicted wavelength of faulted topography is controlled by lithospheric structure, correlating negatively with spreading rate (Fig. 1). In contrast, at periods greater than the threshold, the fault wavelengths are directly controlled by the period of the magmatic–amagmatic cycle and hence correlate positively with spreading rate (19, 21). At intermediate spreading rates and faster, the positive correlation is predicted for the 100-yr climate period but not for the 41-kyr period ; at fast spreading rates, the prediction of the positive correlation includes the ~41ky period. Hence the models provide a physics-based explanation for the observations.

An interesting result is that the 100-kyr signal was not detected in the topography at the fast spreading rates (6). One should consider, first, that such a long period of sea level change would result in a minimal rate of pressure change in the melting zone and, second, that the background rate of decompression melting is maximal at the fast spreading rates, and, therefore, the proportional change in magma flux to the ridge axis would be small (12). That said, signals in seafloor topography corresponding to periods close to 100 ky have been documented by previous studies at two locations of fast spreading (15, 16). One complication is that the form of extensional faulting simulated in the models is least common at fast-spreading environments (22). An alternative form of faulting that is more common at fast-spreading ridges occurs due to the downward collapse of the seafloor overlying the magmatic center of the ridge axis during periods of low or waning magmatism (23). Nonetheless, this alternative form of faulting could also explain the observations if it, too, is controlled by the fluctuating magma flux associated with climate cycles. Finally, undulations in the thickness of the oceanic crust, reflecting oscillations in magma flux, have been found to correspond approximately to the 100-kr and 41-ky periods at one fast-spreading location (16), however, the relationship between those undulations and faulting was not thoroughly examined.

The findings of Huybers et al. (6) motivate more focused attention on the fast spreading rates for further investigations of how climate may have impacted the formation of the oceanic crust. As seafloor topography records many millions of years of geologic history, it is tantalizing to imagine the possibility that the seafloor record can inform us about climate that far back in the past. The study also energizes the question of how significantly magmatic outgassing can influence atmospheric CO_2 and promote two-way feedback between the solid earth and the climate system (24, 25). The study strengthens the evidence that the different Earth systems have consequential interconnections across many levels and timescales, and stimulates an integrative systems approach to the reasoning and exploration in the geosciences.

ACKNOWLEDGMENTS. G.I. was supported by grant NSF-OCE-1928804.

1. E. S. Kappel, W. B. F. Ryan, Volcanic episodicity and a non-steady state rift valley along the northeast Pacific spreading centers: Evidence from Sea MARC I. *J. Geophys. Res.* **91**, 13,925–13,940 (1986).
2. K. C. Macdonald, Mid-ocean ridges: Fine scale tectonic volcanic and hydrothermal processes within the plate boundary zone. *Annu. Rev. Earth Planet. Sci.* **10**, 155–190 (1982).
3. W. Thatcher, D. P. Hill, A simple model for the fault-generated morphology of slow-spreading mid-oceanic ridges. *J. Geophys. Res.* **100**, 561–570 (1995).
4. J. A. Olive, P. Dublanchet, Controls on the magmatic fraction of extension at mid-ocean ridges. *Earth Planet. Sci. Lett.* **549**, 116541 (2020).

5. R. Parnell-Turner, S. J. Sim, J. A. Olive, Time-dependent crustal accretion on the Southeast Indian Ridge revealed by Malaysia Airlines Flight MH370 search. *Geophys. Res. Lett.* **47**, e2020GL087349 (2020).
6. P. Huybers *et al.*, Influence of Late Pleistocene sea level variations on midocean ridge spacing in faulting simulations and a global analysis of bathymetry. *Proc. National Acad. Sci. U.S.A.*, 10.1073/pnas.2204761119 (2022)
7. M. A. Jellinek *et al.*, Did melting glaciers cause volcanic eruptions in eastern California? Probing the mechanics of dike formation. *J. Geophys. Res.* **109**, B09206 (2004).
8. P. Huybers, C. Langmuir, Feedback between deglaciation, volcanism, and atmospheric CO_2. *Earth Planet. Sci. Lett.* **286**, 479–491 (2009).
9. S. F. L. Watt *et al.*, The volcanic response to deglaciation: Evidence from glaciated arcs and a reassessment of global eruption records. *Earth Sci. Rev.* **122**, 77–102 (2013).
10. D. C. Lund, P. D. Asimow, Does sea level influence mid-ocean ridge magmatism on Milankovitch timescales? *Geochem. Geophys. Geosys.* **12**, Q12009 (2011).
11. D. C. Lund *et al.*, Enhanced East Pacific Rise hydrothermal activity during the last two glacial terminations. *Science* **351**, 478–482 (2016).
12. J. W. Crowley, R. F. Katz, P. Huybers, C. H. Langmuir, S. H. Park, Glacial cycles drive variations in the production of oceanic crust. *Science* **347**, 1237–1240 (2015).
13. J. A. Goff *et al.*, No evidence for Milankovitch cycle influence on abyssal hills at intermediate, fast, and superfast spreading rates. *Geophys. Res. Lett.* **45**, 10,305–10,313 (2018).
14. P. Huybers *et al.*, Comment on "Sensitivity of seafloor bathymetry to climate-driven fluctuations in mid-ocean ridge magma supply." *Science* **352**, 1405 (2016).
15. M. Tolstoy, Mid-ocean ridge eruptions as a climate valve. *Geophys. Res. Lett.* **42**, 1346–1351 (2015).
16. B. Boulahanis *et al.*, Do sea level variations influence mid-ocean ridge magma supply? A test using crustal thickness and bathymetry data from the East Pacific Rise. *Earth Planet. Sci. Lett.* **535**, 116121 (2020).
17. J.-A. Olive *et al.*, Response to Comment on "Sensitivity of seafloor bathymetry to climate-driven fluctuations in mid-ocean ridge magma supply." *Science* **352**, 1405 (2016).
18. J. A. Goff, Y. Ma, A. Shah, J. R. Cochran, J. C. Sempéré, Stochastic analysis of seafloor morphology on the flank of the Southeast Indian Ridge: The influence of ridge morphology on the formation of abyssal hills. *J. Geophys. Res.* **102**, 15,521–15,534 (1997).
19. J. A. Olive *et al.*, Sensitivity of seafloor bathymetry to climate-driven fluctuations in mid-ocean ridge magma supply. *Science* **350**, 310–313 (2015).
20. J. A. Goff, Comment on "Glacial cycles drive variations in the production of oceanic crust." *Science* **349**, 1065 (2015).
21. G. Ito, M. D. Behn, Magmatic and tectonic extension at mid-ocean ridges: 2. Origin of axial morphology. *Geochem. Geophys. Geosys.* **9**, Q09O12 (2008).
22. S. M. Carbotte, K. C. Macdonald, Causes of variation in fault-facing direction on the ocean floor. *Geology* **18**, 749–752 (1990).
23. M. H. Cormier *et al.*, Waxing and waning volcanism along the East Pacific Rise on a millennium time scale. *Geology* **31**, 633–636 (2003).
24. W. S. Broecker *et al.*, Two contributors to the glacial CO_2 decline. *Earth Planet. Sci. Lett.* **429**, 191–196 (2015).
25. J. Hasenclever *et al.*, Sea level fall during glaciation stabilized atmospheric CO_2 by enhanced volcanic degassing. *Nat. Commun.* **8**, 15867 (2017).